

# FLYING LASER SPOT THERMAL WAVE IR IMAGING

Y.Q. Wang, P.Chen, P.K. Kuo, L.D. Favro, and R.L. Thomas

Department of Physics and Institute for Manufacturing Research  
Wayne State University, Detroit, MI 48202

## INTRODUCTION

In a previous report, some of the authors have described the basic experimental technique for flying laser spot thermal wave IR imaging, and demonstrated its potential usefulness for the detection of closed vertical cracks [1]. The objective of the present work is to provide a theoretical description of the temperature distribution from a Gaussian-shaped surface heat spot, scanned at constant speed, and to compare the predictions of that theoretical description with temperature distributions measured experimentally with our thermal wave flying spot imaging system.

## THEORY

The measured temperature profile,  $\tilde{T}$  of the moving laser spot is the convolution of temperature distribution,  $T$ , from a moving Gaussian source with a detector response function,  $D$ , (neglecting the heat loss from samples):

$$\tilde{T}(v, \alpha, w_s, w_d) = T(\vec{r}, t, v, \alpha, w_s) \otimes D(\vec{r}, t, w_d). \quad (1)$$

Here,  $v$  represents the source speed,  $\alpha$  the thermal diffusivity of the material, and  $w_s$  and  $w_d$  represent the Gaussian radii of the source spot and the half width of the detector spot, respectively. The temperature distribution from the moving source can be written as

$$T(\vec{r}, t, v, \alpha, w_s) = \frac{1}{\rho c} \int_{t_0}^t dt' \int d^3\vec{r}' G(\vec{r}, \vec{r}', t, t') f(\vec{r}', t'), \quad (2)$$

where  $\rho$  is the mass density and  $c$  the specific heat capacity of the sample, respectively, and where the Green's function,  $G$ , and the source function,  $f$ , are given by

$$G(\vec{r}, \vec{r}', t, t') = \left[ \frac{1}{4\pi\alpha(t-t')} \right]^{\frac{3}{2}} e^{-\frac{(\vec{r} - \vec{r}')^2}{4\alpha(t-t')}}, \text{ and} \quad (3)$$

$$f(\vec{r}, t) = \frac{Q}{\pi w_s} e^{-\frac{(x - vt)^2 + y^2}{w_s^2}} \delta(z). \quad (4)$$

The detector response function,  $D$ , is given by

$$D = \begin{cases} 1 & \text{for } (x_0 + w_d) \leq x \leq (x_0 - w_d) \\ & \text{and } (y_0 + w_d) \leq y \leq (y_0 - w_d) \\ 0 & \text{otherwise.} \end{cases} \quad (5)$$

Using Eqs. 1-5, we have calculated the temperature profiles of the moving heating spot as a function of the separation,  $\Delta x$ , between the heating spot and the detector spot for a material with a thermal diffusivity,  $\alpha = 0.085 \text{ cm}^2/\text{s}$ , and for spot speeds varying from 3.3 m/s to 20.5 m/s. The assumed source and detector sizes are  $w_s = 53 \mu\text{m}$  and  $w_d = 60 \mu\text{m}$ , respectively. The results of our calculation are shown in Fig. 1.

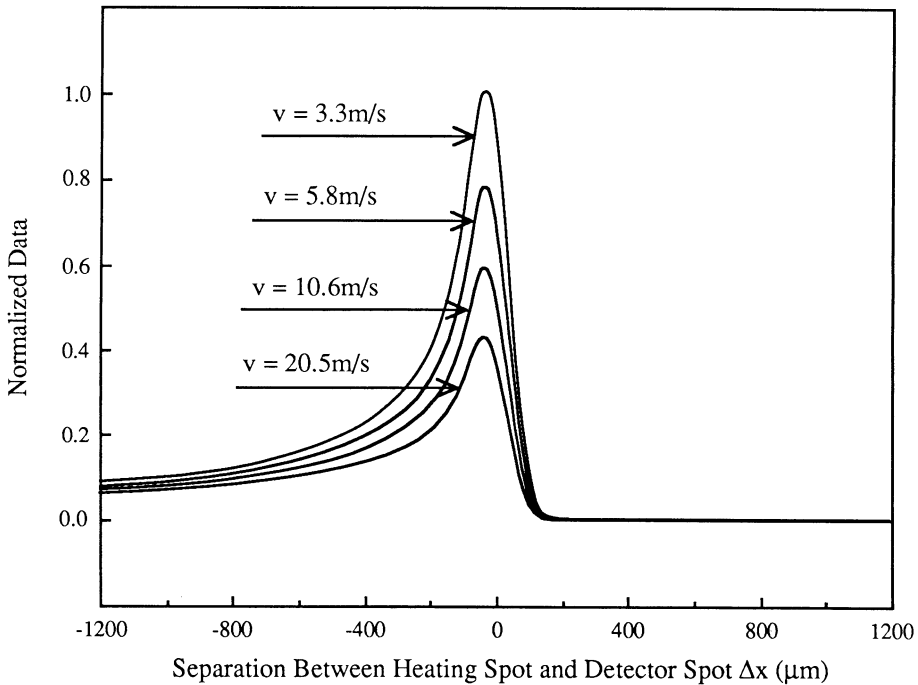


Fig. 1. Temperature profiles of the moving heating spot as a function of the separation,  $\Delta x$ , between the heating spot and the detector spot for a material with a thermal diffusivity,  $\alpha = 0.085 \text{ cm}^2/\text{s}$ , and for spot speeds varying from 3.3 m/s to 20.5 m/s. The assumed source and detector sizes are  $w_s = 53 \mu\text{m}$  and  $w_d = 60 \mu\text{m}$ , respectively.

## EXPERIMENT

The block diagram of the system used to carry out the thermal wave flying spot experiments is shown in Fig. 2. The detector control system is used to scan the separation,  $\Delta x$ , between the heating spot and the detector spot, and the x-scanner is used to set the constant speeds,  $v$ , corresponding to the assumptions used in generating the theoretical curves displayed in Fig. 1.

A series of experimental temperature profiles for a graphite specimen ( $\alpha \approx 0.085 \text{ cm}^2/\text{s}$ ), for several spot speeds are plotted in the same fashion as were the theoretical predictions displayed in Fig. 1. It can be seen that there is good qualitative agreement between theory (Fig. 1) and experiment (Fig. 3).

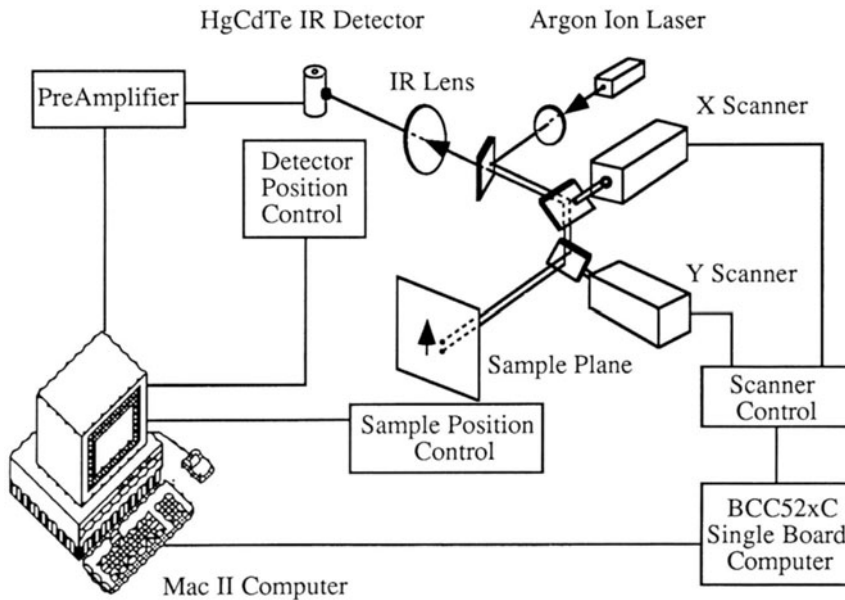


Fig. 2. Block diagram of the system used to carry out the thermal wave flying spot experiments. The detector control system is used to scan the separation,  $\Delta x$ , between the heating spot and the detector spot, and the x-scanner is used to set the constant speeds,  $v$ , corresponding to the assumptions used in generating the theoretical curves displayed in Fig. 1.

## CONCLUSIONS

The theoretical and experimental basis for flying laser spot thermal wave IR imaging is now a firm footing. Good qualitative agreement exists between theory and experiment, and it is expected that further refinement of both theory and experiment could make this a useful technique for measuring thermal properties (e.g., for determining the thermal diffusivities of materials).

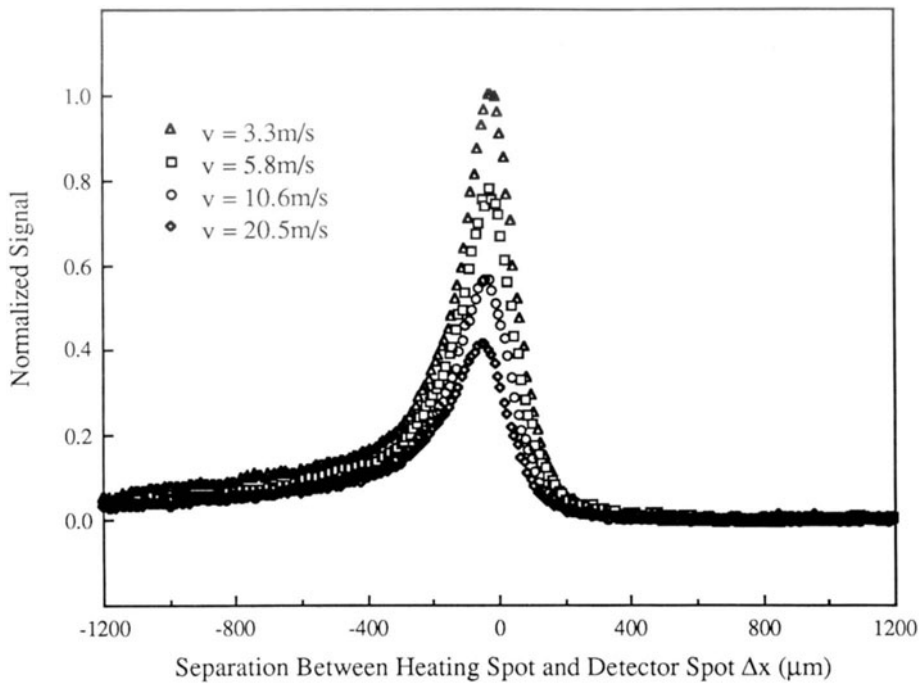


Fig. 3. Experimental temperature profiles for a graphite specimen ( $\alpha \cong 0.085 \text{ cm}^2/\text{s}$ ), for several spot speeds are plotted in the same fashion as were the theoretical predictions displayed in Fig. 1.

#### ACKNOWLEDGEMENTS

This work was sponsored by the Army Research Office, under Contract No. DAAL-03-88-K-0089, and by the Institute for Manufacturing Research, Wayne State University.

#### REFERENCES

1. Y.Q. Wang, P.K. Kuo, L.D. Favro, and R.L. Thomas, Review of Progress in Quantitative NDE, Vol. 9A, (Plenum Press, New York, 1990), p. 511.